Entanglement beating in a cavity optomechanical system under two-field driving

Chang-Sheng Hu, Zhi-Qiang Liu, Ye Liu, Li-Tuo Shen, Huaizhi Wu,* and Shi-Biao Zheng†
Fujian Key Laboratory of Quantum Information and Quantum Optics and Department of Physics, Fuzhou University, Fuzhou 350116, People's Republic of China

(Received 20 October 2019; accepted 12 February 2020; published 10 March 2020)

An optomechanical cavity driven by a periodically amplitude-modulated laser can generate steady light-mechanical entanglement with time periodicity. Similar results can be alternatively obtained by pumping an especially tuned optical degenerate parametric amplifier (DPA) inside the cavity. While the two laser beams are simultaneously applied, the optomechanical entanglement can exhibit constructive and destructive interference patterns, depending on their cooperative phase, which further gives rise to beating in entanglement dynamics if the two modulation frequencies are slightly different, followed by a beating frequency-dependent dynamical behavior in the energy exchange between light and a mechanical oscillator. The optimal dynamical entanglement goes beyond what is attainable by the scenario with two superimposed cavity drivings, as a result of the specially DPA-modulated quantum dynamics. Moreover, we calculate correlation spectra between the cavity and mechanical modes, and we find correspondence between the light-oscillator entanglement and the correlation spectra under the cooperative effect. The cooperation-enhanced optomechanical entanglement is robust against the thermal temperature, and is potentially useful for continuous variable quantum information processing.

DOI: 10.1103/PhysRevA.101.033810

I. INTRODUCTION

Entanglement is a fundamental feature of quantum mechanics and an essential resource for quantum communication and information processing. Although many quantum information protocols exploit entangled qubits with a well-defined and anharmonic discrete state space, the original Einstein-Podolsky-Rosen [1] entanglement involves continuous variables (CVs), and CV entanglement has many modern applications [2–8]. A standard cavity optomechanical setup [9–13], which builds on the radiation-pressure-force induced coupling between the cavity field and a mechanical resonator (i.e., two harmonic oscillators), is an ideal candidate for studying CV entanglement. The light-mechanical entanglement provides opportunities for a fundamental test of quantum theory [14–18], quantum information storage, and construction of quantum networks [19–22]. Moreover, generalization of the standard setup to a multimode scenario allows us to study entanglement of multiple optical fields and mechanical modes [23–33].

An optomechanical system subject to parametric modulation offers a promising platform for enhancement of quantum effects, such as generation of nonclassical macroscopic states [34,35], implementation of strong mechanical squeezing [36–43], and improvement of quantum entanglement [44–50]. By introducing amplitude-modulated drivings to the standard optomechanical cavity, which are widely used in Rydberg atoms [51] and oscillating molecules [52], Mari and Eisert [36,44] have proved that the stationary entanglement between the cavity field and the mechanical resonator can be significantly improved, and the degree of mechanical squeezing can be greatly enhanced and can approach the 3-dB limit. Instead, by parametrically modulating the spring constant of the mechanical resonator, the modified optomechanical setup can be used to generate optical amplification and squeezing [37–40].

Furthermore, an optomechanical system involving more than one mechanical resonator can be modulated by introducing a directly time-dependent coupling between the mechanical oscillators, leading to strong entanglement for the macroscopic objects [47,48]. The following question then arises: Can two independent modulations simultaneously applied be cooperative? The first attempt by Farace and Giovannetti [53] combined both amplitude-modulated cavity driving and parametric mechanical driving, and it showed that the quantum interference between the two independent modulations can improve mechanical squeezing and cooling, but has almost no impact on the cooperative effects of light-mechanical entanglement.

An optical degenerate parametric amplifier (DPA), which is placed inside the optomechanical cavity and is pumped by an external laser, can directly lead to optical amplification and is able to modulate the optomechanical coupling in a way analogous to periodic cavity driving [41,42,50]. The utilization of DPA can help to achieve strong mechanical cooling and squeezing [41,54], and increase the single-photon optomechanical coupling strength up to the strong-coupling regime [55]. In a recent paper [43], we have shown that when the DPA-assisted optomechanical setup is driven by an amplitude-modulated laser, twofold mechanical squeezing can be realized due to the cooperative effect of the two laser drivings, which sets up a good example of cooperatively independent two-field modulations.

In this paper, we examine the cooperative effect of two-field driving on light-mechanical entanglement. The cooperative effect between the cavity driving and the DPA pumping can be found in both the classical and quantum regimes,

*huaizhi.wu@fzu.edu.cn
†sbzheng11@163.com

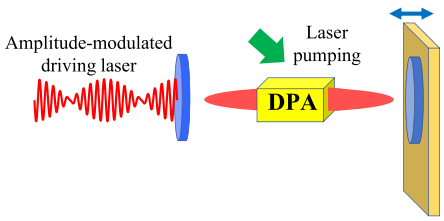

FIG. 1. Schematic of the setup: An optical DPA is placed inside the standard optomechanical cavity and is pumped by a laser field. The cavity is driven by a periodically amplitude-modulated laser.

leading to enhancement and beating in light-mechanical entanglement. Our results are quite remarkable based on the following facts. First, the dynamical light-mechanical entanglement can be well controlled by the phase difference of the two independent laser drivings, giving rise to nicely in-phase and out-of-phase interference patterns in the entanglement dynamics. Similar results were widely studied in discrete qubit systems [56–59]. The result here is particularly interesting since the optomechanical entanglement is greatly enhanced in contrast to the case under two classical cavity drivings. Second, when the effective modulation frequencies of the two driving fields are slightly different, a beat pattern known as the typical phenomenon of two-wave interference occurs in the light-mechanical entanglement. The beat frequency is exactly given by the absolute value of the difference in modulation frequency of the two driving fields. Due to the entanglement beating, the energy transfer between the cavity mode and the mechanical resonator exhibits an oscillatory dynamics with the envelope of the frequency precisely equal to the beat frequency. Therefore, the dynamical light-mechanical entanglement gives a direct demonstration of the cooperative effect of two independent modulations. The optomechanical setup under two-field driving thus provides new possibilities for heralded phase control of light-mechanical entanglement and may find practical applications in CV quantum information processing and communications.

The rest of the paper is organized as follows: In Sec. II, we introduce the DPA-assisted optomechanical system with the cavity being driven by an amplitude-modulated laser. In Sec. III, we introduce the cross correlation and the logarithmic negativity for measuring the quantum correlations between the cavity and mechanical modes. In Sec. IV, we present how the quantum correlations are cooperatively modulated by the DPA pumping and the amplitude-modulated driving laser without thermal noise, and we show entanglement beating in the dynamical behavior. The effect of a finite thermal temperature is finally considered. Conclusions and general remarks follow in Sec. V. Additional technical derivations are shown in the Appendixes.

II. THE MODEL

We consider a degenerate optical parametric amplifier (DPA) inside a Fabry-Pérot cavity with one fixed partially transmitting mirror and one movable totally reflecting mirror, as shown in Fig. 1. The spatial distance between the two mirrors is L. The movable mirror is treated as a quantum-mechanical harmonic oscillator with effective mass m, frequency ω_m, and mechanical quality factor Q, leading to a mechanical damping rate $\gamma_m = \omega_m/Q$. The cavity mode of the resonance frequency ω_c is driven by an amplitude-modulated input laser of the carrier frequency ω_l and the driving strength $\epsilon(t) = \epsilon_0 + 2\epsilon_1 \cos(\Omega t - \varphi)$ with $\epsilon_1/\epsilon_0 < 1$, where $\epsilon_n = \sqrt{2\kappa P_n/(\hbar\omega_l)}$ $(n = 0, 1)$ depends on the laser power $\{P_n\}$, with $\kappa = c\pi/(2FL)$ being the cavity decay rate and relating to the cavity finesse F, the cavity length L, and the speed of light c; Ω and φ are the modulation frequency and the initial phase of the driving laser, respectively. The optical DPA is pumped by a coherent field at frequency $2\omega_p$, leading to the generation of pairs of down-converted photons. The Hamiltonian of the system in the rotating frame at the laser frequency ω_l can be written as

$$H = \hbar\Delta_0 a^\dagger a + \hbar\omega_m b^\dagger b - \hbar g a^\dagger a(b + b^\dagger) + i\hbar[\epsilon(t)a^\dagger - \epsilon^*(t)a] + i\hbar\Lambda(e^{i\theta}a^{\dagger 2}e^{-i\Delta_p t} - e^{-i\theta}a^2 e^{i\Delta_p t}), \quad (1)$$

where $\Delta_0 = \omega_c - \omega_l$ and $\Delta_p/2 = \omega_p - \omega_l$ are detunings of the laser driving from the cavity resonance ω_c and the degenerate photonic frequency ω_p, respectively; a $(a^\dagger)$ and b $(b^\dagger)$ are the annihilation (creation) operators for the cavity and mechanical modes. The third term describes the light-oscillator radiation pressure interaction with the single-photon coupling strength $g = x_{\rm ZPF}\omega_c/L$, where $x_{\rm ZPF} = \sqrt{\hbar/2m\omega_m}$ is the zero-point motion of the mechanical mode. The fourth term represents the modulated laser driving along the axis of the cavity. The last term shows the DPA pumping with the gain Λ related to the pumping power and the laser phase θ.

By including the thermal noises with respect to the optical and mechanical modes, we can analyze the time-evolutional dynamics of the optomechanical system via the set of quantum Langevin equations [60]:

$$\begin{aligned}\dot{a} &= -(\kappa + i\Delta_0)a + iga(b + b^\dagger) + \epsilon(t) \\ &\quad + 2\Lambda e^{i\theta}a^\dagger e^{-i\Delta_p t} + \sqrt{2\kappa}a_{in}(t), \\ \dot{b} &= -i\omega_m b + iga^\dagger a - \frac{\gamma_m}{2}b + \sqrt{\gamma_m}b_{in}(t), \end{aligned} \quad (2)$$

where $a_{in}(t)$ and $b_{in}(t)$ are zero-mean value operators, describing the cavity vacuum input noise and the mechanical noise, respectively, which satisfy the Markovian correlation functions $\langle a_{in}(t)a_{in}^\dagger(t')\rangle = \delta(t - t')$, $\langle b_{in}^\dagger(t)b_{in}(t')\rangle = n_m\delta(t - t')$ with the cavity being at zero temperature and $n_m = [\exp(\hbar\omega_m/k_BT) - 1]^{-1}$ being the mean number of thermal excitations of the mechanical mode at the thermal temperature T [60].

III. MEASUREMENTS OF CROSS-CORRELATIONS AND QUANTUM ENTANGLEMENT

We study the quantum properties of the system, the cross-correlation, and the quantum entanglement between the optical and mechanical modes through the quantum fluctuations around the steady-state classical mean values $\langle O\rangle(t)$ $(O = a, b)$, i.e., $a = \langle a\rangle + \delta a$ and $b = \langle b\rangle + \delta b$, where δO are quantum fluctuation operators with zero mean, and the cavity intensity is assumed to be $|\langle a\rangle|^2 \gg 1$. The equations of motion for the quantum operators after linearization are given by

($\hbar = 1$)

$$\begin{aligned}\delta\dot{a} &= -i\Delta(t)\delta a + iG(t)(\delta b^\dagger + \delta b)\\ &\quad + 2\Lambda e^{i\theta}\delta a^\dagger e^{-i\Omega t} - \kappa\delta a + \sqrt{2\kappa}a_{in}(t),\\ \delta\dot{b} &= -i\omega_m\delta b + i[G(t)\delta a^\dagger + G^*(t)\delta a]\\ &\quad - \frac{\gamma_m}{2}\delta b + \sqrt{\gamma_m}b_{in}(t),\end{aligned} \tag{3}$$

where $\Delta_p = \Omega$ is set such that the system is periodically modulated by the DPA pumping at the exact same frequency as that of the modulated cavity driving, $\Delta(t) = \Delta_0 + \bar{\delta}$ [with $\bar{\delta} \equiv -g\langle b(t) + b^\dagger(t)\rangle$] is the effective detuning of the cavity resonance from the driving laser frequency slightly modulated by the mechanical motion, and $G(t) = g\langle a(t)\rangle$ represents the effective optomechanical coupling strength related to the cavity intensity.

We study the semiclassical dynamics of the modulated system in the long-time limit, where the asymptotically dynamical steady state evolves toward a fixed orbit with a period being equal to the modulation period of the cavity driving $\tau = 2\pi/\Omega$. In this case, the asymptotic solution of the classical values $\langle a(t)\rangle$, $\langle q(t)\rangle$, and $\langle p(t)\rangle$ can be approximately given by the Fourier expansion, $\langle O\rangle(t) = \sum_{j=0}^{\infty}\sum_{n=-\infty}^{\infty} O_{n,j}(\sqrt{2}g)^j e^{in\Omega t}$ (see Appendix A). For $\Lambda \ll \Delta, \Omega$, the cavity field, which is in the zeroth-order in g, can be approximately written as

$$\begin{aligned}\langle a(t)\rangle \approx{}& \frac{\epsilon_0}{\kappa + i\Delta_0} + \frac{\epsilon_1 e^{-i(\Omega t-\varphi)}}{\kappa + i(\Delta_0 - \Omega)}\left[1 + \frac{2\Lambda\epsilon_0 e^{i(\theta-\varphi)}}{\epsilon_1(\kappa - i\Delta_0)}\right]\\ &+ \frac{\epsilon_1 e^{i(\Omega t-\varphi)}}{\kappa + i(\Delta_0 + \Omega)},\end{aligned} \tag{4}$$

where we have omitted the terms oscillating at higher sideband frequencies $n\Omega t$ ($n \geqslant 2$). For $\Lambda = 0$, the first term in Eq. (4) is the cavity field under the constant driving ϵ_0, while the second and third terms ($\sim\epsilon_1$) describe the effect of the periodic modulation. Note that the amplitude-modulated driving $\epsilon(t) = \epsilon_0 + \epsilon_1 e^{-i(\Omega t-\varphi)} + \epsilon_1 e^{i(\Omega t-\varphi)}$ is equivalent to cavity drivings of three different tones, and without the optomechanical coupling the classical value $\langle a(t)\rangle$ linearly responding to the three-tone drivings can thus only include three frequency components "0", "$-\Omega$," and "$+\Omega$." On the other hand, the DPA pumping detuned from the carrier frequency of the cavity driving (i.e., the frequency component "0") plays a similar role to the modulation of the driving amplitude of the frequency component "$-\Omega$"; see Eq. (2). Thus, the linear response of $\langle a(t)\rangle$ to different driving components can be independently derived, and the DPA has no effect on the frequency component "$+\Omega$." As a result, the DPA pumping, in the classical regime, can cooperatively enhance or weaken the modulation depending on the cooperative phases $\Delta\phi \equiv \theta - \varphi$ and the relative driving strength, e.g., for $\Delta\phi = \pi + \arg(\kappa - i\Delta_0)$ and $2\Lambda\epsilon_0/\sqrt{\kappa^2 + \Delta_0^2} = \epsilon_1$, the component of $\langle a(t)\rangle$ in frequency $-\Omega$ can be completely eliminated, corresponding to classical interference of two superposition fields. For a more generic case involving the nonlinear optomechanical interaction, the optomechanical coupling strength can therefore be effectively expanded as (see Appendix A) [43]

$$G(t) = g_0 + g_1 e^{-i\Omega t} + g_{-1}e^{i\Omega t}, \tag{5}$$

where $g_n = (1/\sqrt{2})\sum_{j=0}^{\infty} a_{-n,j}(\sqrt{2}g)^{j+1}$ with $n = -1,\ 0,$ and 1.

We assume that the cavity driving is set close to the red sideband $\Delta \simeq \omega_m$, and its amplitude is modulated at the frequency $\Omega = 2\omega_m$. Then, by performing a transformation to a frame rotating at the mechanical frequency ω_m (i.e., $\delta\tilde{O} = \delta O e^{i\omega_m t}$ and $\tilde{O}_{in} = O_{in}e^{i\omega_m t}$) and considering the parameter regime $\omega_m \gg |g_n|,\ \kappa, 2\Lambda$, we obtain the reduced form of Eq. (3) under the rotating-wave approximation,

$$\begin{aligned}\delta\dot{\tilde{a}} &= -i\bar{\delta}\delta\tilde{a} + ig_0\delta\tilde{b} + ig_1\delta\tilde{b}^\dagger + 2\Lambda e^{i\theta}\delta\tilde{a}^\dagger\\ &\quad - \kappa\delta\tilde{a} + \sqrt{2\kappa}\tilde{a}_{in}(t),\\ \delta\dot{\tilde{b}} &= ig_0^*\delta\tilde{a} + ig_1\delta\tilde{a}^\dagger - \frac{\gamma_m}{2}\delta\tilde{b} + \sqrt{\gamma_m}\tilde{b}_{in}(t).\end{aligned} \tag{6}$$

Note that the terms with respect to "$+\Omega$" and even higher-frequency components in the optomechanical coupling strength are always far from the cavity resonance and have weak amplitudes, thus the quantum dynamics of the system and the optomechanical entanglement will be dominated by the two driving frequency components "0" and "$-\Omega$." We then take the Fourier transform of Eq. (6) and express the fluctuation operators for cavity and mechanical modes in the frequency domain as

$$\begin{aligned}\tilde{a}(\omega) &= A_1(\omega)\tilde{a}_{in}(\omega) + B_1(\omega)\tilde{a}_{in}^\dagger(\omega)\\ &\quad + C_1(\omega)\tilde{b}_{in}(\omega) + D_1(\omega)\tilde{b}_{in}^\dagger(\omega),\end{aligned} \tag{7}$$

$$\begin{aligned}\tilde{b}(\omega) &= A_2(\omega)\tilde{a}_{in}(\omega) + B_2(\omega)\tilde{a}_{in}^\dagger(\omega)\\ &\quad + C_2(\omega)\tilde{b}_{in}(\omega) + D_2(\omega)\tilde{b}_{in}^\dagger(\omega),\end{aligned} \tag{8}$$

where

$$\begin{aligned}A_1(\omega) &= \frac{\sqrt{2\kappa}}{d(\omega)}\{v(\omega)^2[u(\omega) - i\bar{\delta}] + |g_{01}|^2 v(\omega)\},\\ B_1(\omega) &= \frac{\sqrt{2\kappa}}{d(\omega)}2\Lambda e^{i\theta}v(\omega)^2,\\ C_1(\omega) &= \frac{i\sqrt{\gamma_m}}{d(\omega)}\{g_0 v(\omega)[u(\omega) - i\bar{\delta}] + g_0|g_{01}|^2\\ &\quad - 2\Lambda g_1^* e^{i\theta}v(\omega)\},\\ D_1(\omega) &= \frac{i\sqrt{\gamma_m}}{d(\omega)}\{g_1 v(\omega)[u(\omega) - i\bar{\delta}] + g_1|g_{01}|^2\\ &\quad - 2\Lambda g_0^* e^{i\theta}v(\omega)\},\\ A_2(\omega) &= \frac{i\sqrt{2\kappa}}{d(\omega)}\{g_0^* v(\omega)[u(\omega) - i\bar{\delta}] + g_0^*|g_{01}|^2\\ &\quad + 2\Lambda g_1 e^{-i\theta}v(\omega)\},\\ B_2(\omega) &= \frac{i\sqrt{2\kappa}}{d(\omega)}\{g_1 v(\omega)[u(\omega) + i\bar{\delta}] + g_1|g_{01}|^2\\ &\quad + 2\Lambda g_0^* e^{i\theta}v(\omega)\},\\ C_2(\omega) &= \frac{\sqrt{\gamma_m}}{d(\omega)}\{v(\omega)[u(\omega)^2 + \bar{\delta}^2 - 4\Lambda^2] + |g_0|^2[u(\omega) + i\bar{\delta}]\end{aligned}$$

$$- |g_1|^2[u(\omega) - i\bar{\delta}] - 2\Lambda(g_0 g_1 e^{-i\theta} - g_0^* g_1^* e^{i\theta})\},$$

$$D_2(\omega) = \frac{2\sqrt{\gamma_m}}{d(\omega)}(-\Lambda g_1^2 e^{-i\theta} + i\bar{\delta} g_0^* g_1 + \Lambda g_0^{*2} e^{i\theta}),$$

with $u(\omega) = \kappa - i\omega$, $v(\omega) = \frac{\gamma_m}{2} - i\omega$, $|g_{01}|^2 = |g_0|^2 - |g_1|^2$, and $d(\omega) = [u(\omega)v(\omega) + |g_{01}|^2]^2 + (\bar{\delta}^2 - 4\Lambda^2)v(\omega)^2$. By using noise correlation functions $\langle \tilde{a}_{in}(\omega)\tilde{a}_{in}^\dagger(-\omega')\rangle = 2\pi\delta(\omega + \omega')$ and $\langle \tilde{b}_{in}(\omega)\tilde{b}_{in}^\dagger(-\omega')\rangle = 2\pi(n_m + 1)\delta(\omega + \omega')$, we finally obtain the cross-correlation spectra $S(\omega) = \langle a(\omega)b(\omega)\rangle/2\pi$ for the cavity and mechanical modes [29,61,62], i.e.,

$$S(\omega) = A_1(\omega)B_2(\omega) + (n_m + 1)C_1(\omega)D_2(\omega) + n_m D_1(\omega)C_2(\omega). \tag{9}$$

To quantify the degree of light-oscillator entanglement, we first introduce the amplitude and phase quadratures of the cavity mode $\delta x = (\delta a + \delta a^\dagger)/\sqrt{2}$, $\delta y = -i(\delta a - \delta a^\dagger)/\sqrt{2}$, the position and momentum quadratures of the mechanical mode $\delta q = (\delta b + \delta b^\dagger)/\sqrt{2}$, $\delta p = -i(\delta b - \delta b^\dagger)/\sqrt{2}$, and the analogous input quantum noise quadratures $\delta x_{in} = (\delta a_{in} + \delta a_{in}^\dagger)/\sqrt{2}$, $\delta y_{in} = -i(\delta a_{in} - \delta a_{in}^\dagger)/\sqrt{2}$. Then, the quantum Langevin equations for the quadrature operators $u(t) = [\delta q, \delta p, \delta x, \delta y]^T$ derived from Eq. (3) are given by

$$\dot{u}(t) = M(t)u(t) + n(t), \tag{10}$$

where $M(t) = M_0(t) + M_1(t)$ is the drift matrix with

$$M_0(t) = \begin{bmatrix} 0 & \omega_m & 0 & 0 \\ -\omega_m & -\gamma_m & 2G_x(t) & 2G_y(t) \\ -2G_y(t) & 0 & -\kappa & \Delta \\ 2G_x(t) & 0 & -\Delta & -\kappa \end{bmatrix} \tag{11}$$

and

$$M_1(t) = \begin{bmatrix} 0 & 0 & 0 & 0 \\ 0 & 0 & 0 & 0 \\ 0 & 0 & \kappa_c(t) & -\Delta_s(t) \\ 0 & 0 & -\Delta_s(t) & -\kappa_c(t) \end{bmatrix}, \tag{12}$$

$n(t) = [0, \xi(t), \sqrt{2\kappa}\delta x_{in}, \sqrt{2\kappa}\delta y_{in}]^T$ is the diffusion corresponding to noise sources, $G(t) = G_x(t) + iG_y(t)$, $\Delta_s(t) = 2\Lambda\sin(\Omega t - \theta)$, $\kappa_c(t) = 2\Lambda\cos(\Omega t - \theta)$, and $\xi(t)$ satisfies $\langle \xi(t)\xi(t') + \xi(t')\xi(t)\rangle/2 = \gamma_m(2n_m + 1)\delta(t - t')$. Note that, in the quantum regime, the effect of the DPA pumping can be found not only in the optomechanical interaction $G(t)$, but also in the coupling between the optical quadratures δx and δy, $\Delta \pm 2\Lambda\sin(\Omega t - \theta)$, as well as the corresponding decay rates $-\kappa \pm 2\Lambda\cos(\Omega t - \theta)$. Thus, the system dynamics induced by the two cooperative drivings and dominated by $M_0(t)$ can be first modulated in a similar way to interference enhancement. Then, the additional quantum effect of the DPA pumping $M_1(t)$ further gives rise to strong modification of the quantum properties of the system.

As the Langevin equations are linear, the initial Gaussian nature of the system can be well preserved for a Gaussian type of noise in a stable system. Thus, we can characterize the second moments of the quadratures of the asymptotic state through the covariance matrix (CM) $V(t)$, with the matrix elements given by

$$V_{k,l}(t) = \langle u_k(t)u_l^\dagger(t) + u_l^\dagger(t)u_k(t)\rangle/2. \tag{13}$$

From Eqs. (10) and (13), we can readily derive a linear differential equation governing the time evolution of $V(t)$,

$$\dot{V}(t) = M(t)V(t) + V(t)M^T(t) + D, \tag{14}$$

with $D = \mathrm{diag}[0, \gamma_m(2n_m + 1), \kappa, \kappa]$ obtained from $D_{k,l}\delta(t - t') = \langle n_k(t)n_l^\dagger(t') + n_l^\dagger(t')n_k(t)\rangle/2$. Thus, the time evolution of the matrix elements $V_{k,l}(t)$ can be inferred from Eq. (14), which comprises of a set of 10 coupled, linear differential equations after removing the repeated elements (e.g., the lower triangular matrix elements), and can be written as

$$\dot{\vec{V}}(t) = \mathcal{L}(t)\vec{V}(t) + \vec{D}, \tag{15}$$

where $\vec{V}(t)$ and $\vec{D}$ are vectors that consist of all 10 elements of the density matrix $V(t)$ and D, respectively. The Liouvillian $\mathcal{L}(t) = \mathcal{I} \otimes M(t) + M(t) \otimes \mathcal{I}$ is a 10×10 matrix, which can be divided into three parts, i.e., $\mathcal{L}(t) = \mathcal{L}_0 + \mathcal{L}_1 + \mathcal{L}_2$, by considering the classically cooperative interaction $\mathcal{L}_0 = \mathcal{I} \otimes M_0(t) + M_0(t) \otimes \mathcal{I}$, the modulation-induced modification of cavity decay rates $\mathcal{L}_1 = \mathrm{diag}[0, 0, \kappa_c, -\kappa_c, 0, \kappa_c, -\kappa_c, 2\kappa_c, 0, -2\kappa_c]$, and the DPA-modulated coupling $\mathcal{L}_2$ between the optical quadratures. The general solution for the linear differential equations (15) is then given by

$$\begin{aligned}\vec{V}(t) &= \int_0^t d\tau [e^{\int_\tau^t dt' \mathcal{L}(t')}]\vec{D} \\ &= \int_0^t d\tau \vec{D} + \int_0^t d\tau \left[\int_\tau^t dt' \mathcal{L}(t')\right]\vec{D} \\ &\quad + \frac{1}{2}\int_0^t d\tau \left[\int_\tau^t dt' \mathcal{L}(t')\right]^2 \vec{D} + \cdots .\end{aligned} \tag{16}$$

If $\mathcal{L}_0$ is time-invariant, the integral $\int_\tau^t dt' \mathcal{L}(t')$ involving just the trigonometry functions can be straightforwardly performed to find all Fourier components of the quantum fluctuations induced solely by the Liouvillian components $\mathcal{L}_1, \mathcal{L}_2$, which can strongly modify the quantum characteristics of the system; see further discussion later. Recalling that the first moments of the mechanical and cavity modes are τ-periodic in the steady state, we can then find that the Liouvillian component $\mathcal{L}_0(t)$, which is related to the classical solutions of $\langle a(t)\rangle$ and $\langle q(t)\rangle$, satisfies $\mathcal{L}_0(t + \tau) = \mathcal{L}_0(t)$. Therefore, the CM is also τ-periodic [i.e., $V(t + \tau) = V(t)$] according to the Floquet theory [36,63]. Finally, we quantify the steady-state light-oscillator entanglement in terms of the logarithmic negativity E_N [64], which can be readily computed from the CM $V(t)$. Consider the following reduced form of the CM:

$$V(t) = \begin{pmatrix} V_1 & V_c \\ V_c^T & V_2 \end{pmatrix}, \tag{17}$$

where V_1, V_2, and V_c are 2×2 subblock matrices of $V(t)$. Then, the logarithmic negativity is given by

$$E_N \equiv \max[0, -\ln 2\eta], \tag{18}$$

with

$$\eta = (1/\sqrt{2})[\Sigma(V) - \sqrt{\Sigma(V)^2 - 4\det(V)}]^{1/2},$$
$$\Sigma(V) = \det(V_1) + \det(V_2) - 2\det(V_c).$$

Note that we can measure the optomechanical entanglement with Eq. (18) only when the system is stable in the long-time limit, which can be further examined by applying the Routh-Hurwitz criterion [65], that is, all the eigenvalues of the matrix $M(t)$ have negative real parts at any time. Thus, the following discussions are based on the fact that the stability condition is well satisfied.

IV. BEATING IN QUANTUM ENTANGLEMENT

There have been studies focusing on the quantum properties of the optomechanical system under multiple-channel modulation [43,53]. Therein, when two independent drivings are simultaneously applied to an optomechanical system, whether the cooperative effect of the two drivings is constructive or detrimental remains questionable. For instance, it has been shown that the enhancement of mechanical quantum squeezing can be achieved with the assistance of DPA pumping [43] or mechanical parametric driving [53]. But the optomechanical entanglement in the latter case cannot benefit from cooperative modulation. Here, we show that the coherent modulation of the optomechanical entanglement with cavity driving and DPA pumping can be witnessed by varying the laser intensities and the cooperative phase $\Delta\phi$.

In Fig. 2, we show the cross-correlation spectra $|\langle S(\omega)\rangle|$ and the corresponding time dependence of the light-oscillator entanglement E_N for different modulation amplitudes ϵ_1, pumping strengths Λ, and cooperative phases $\Delta\phi$. We can see that the amplitude of the cross-correlation spectra grows as ϵ_1 or Λ increases, and strongly relies on the cooperative phase, e.g., the peak values of $|\langle S(\omega)\rangle|$ for $\Delta\phi = \arg(\kappa - i\Delta_0)$ are much larger than that for $\Delta\phi = \pi + \arg(\kappa - i\Delta_0)$. The latter can be further examined in terms of the steady-state optomechanical entanglement, where for a single-field driving, such as $(\epsilon_1, \Lambda)/\omega_m = (2\times10^4, 0)$ or $(\epsilon_1, \Lambda)/\omega_m = (0, 0.04)$, the wavelike dynamical oscillation exhibits translational invariance while ϕ or θ varies from 0 to π and the oscillation amplitude remains unchanged, as shown in Figs. 2(d) and 2(e) (see Appendix B). While both the cavity driving and the DPA pumping are applied, the light-oscillator entanglement E_N can be coherently modulated by the cooperative phase $\Delta\phi$, leading to enhancement or reduction of E_N; see Fig. 2(f).

Furthermore, since the light-oscillator entanglement E_N is periodic in time, we then identify the optimal entanglement with the maximum over one oscillation period τ, i.e., $E_{N,\max} = \max_{\tau}\{E_N(t)\}$ [53]. In Fig. 3, we then show the $\Delta\phi$-dependent cross-correlation area defined as the integral $A = \int_{-\infty}^{+\infty}|S(\omega)|d\omega$ [62] and maximal optomechanical entanglement $E_{N,\max}$ for the system being in the dynamical steady state. We find strong connections between cross-correlation and optomechanical entanglement, evidenced by the similar cooperative-phase dependence of A and $E_{N,\max}$, both of which achieve the maximum at $\Delta\phi = 2k\pi + \Delta\phi_0$ and the minimum at $\Delta\phi = (2k+1)\pi + \Delta\phi_0$ with $\Delta\phi_0 = -0.24\pi$. Note that $\Delta\phi_0$ is different from the classical phase-matching condition

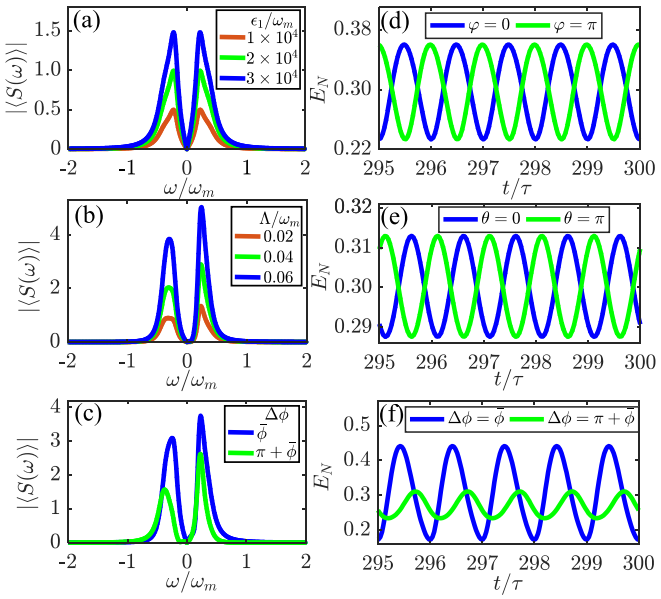

FIG. 2. (a)–(c) Cross-correlation spectra $|S(\omega)|$ vs ω/ω_m. Parameters are (a) $\epsilon_1/\omega_m = 1\times10^4$ [red (gray) line], 2×10^4 [green (light gray) line], and 3×10^4 [blue (dark gray) line] with $\varphi = 0$ and $\Lambda/\omega_m = 0$; (b) $\Lambda/\omega_m = 0.02$ [red (gray) line], 0.04 [green (light gray) line], and 0.06 [blue (dark gray) line] with $\theta = 0$ and $\epsilon_1/\omega_m = 0$; (c) $(\epsilon_1, \Lambda)/\omega_m = (2\times10^4, 0.04)$ with $\Delta\phi = \bar{\phi}$ [blue (dark gray) line] and $\Delta\phi = \pi + \bar{\phi}$ [green (light gray) line]. (d)–(f) Time dependence of light-oscillator entanglement E_N in the long-time limit. Parameters are (d) $(\epsilon_1, \Lambda)/\omega_m = (2\times10^4, 0)$ with $\varphi = 0$ [blue (dark gray) line] and $\varphi = \pi$ [green (light gray) line]; (e) $(\epsilon_1, \Lambda)/\omega_m = (0, 0.04)$ with $\theta = 0$ [blue (dark gray) line] and $\theta = \pi$ [green (light gray) line]; (f) $(\epsilon_1, \Lambda)/\omega_m = (2\times10^4, 0.04)$ with $\Delta\phi = \bar{\phi}$ [blue (dark gray) line] and $\Delta\phi = \pi + \bar{\phi}$ [green (light gray) line], here $\bar{\phi} = \arg(\kappa - i\Delta_0)$. Other parameters are $(\epsilon_0, \Delta_0, g, \kappa, \gamma_m, \bar{\delta}, \Omega, \Delta_p)/\omega_m = (9\times10^4, 1, 2\sqrt{2}\times10^{-6}, 0.2, 10^{-6}, -0.2, 2, 2)$, $n_m = 0$, and $n_a = 0$.

$\sim\arg(\kappa - i\Delta_0)$ since corrections $\bar{\delta}(t)$ induced by optomechanical coupling should be included in the effective detuning $\Delta(t) \approx \Delta_0 - \bar{\delta}_0$, and to first order it is approximately given by

$$\bar{\delta}_0 \approx \frac{2g^2(|a_0|^2 + |a_+|^2)}{\omega_m}, \tag{19}$$

with

$$a_0 = \frac{i2g^2\omega_m a_0|a_+|^2\chi_m^* + \epsilon_0 + 2\Lambda e^{i\theta}a_+^*}{\kappa + i\Delta},$$
$$a_+ = \frac{(K_+^* + i2g^2\omega_m|a_0|^2\chi_m)(\epsilon_1 e^{i\varphi} + 2\Lambda e^{i\theta}a_0^*)}{-4\Delta\omega_m g^2|a_0|^2\chi_m + K_+^*K_-},$$

where $K_\pm = \kappa + i(\Delta \pm \Omega)$ and $\chi_m = 1/(\omega^2 - \Omega^2 - i\gamma_m\Omega)$. As a result, the quantum correlations between the optical field and the mechanical oscillator can be coherently modulated simply by changing the cooperative phase between the cavity driving and the DPA pumping. By adjusting the cooperative phase, the system dynamics dominated by $M_0(t)$ is first phase-locked, similar to interference enhancement of the two individual driving fields. Then, the additional quantum effect of the DPA pumping $M_1(t)$ further gives rise to strong

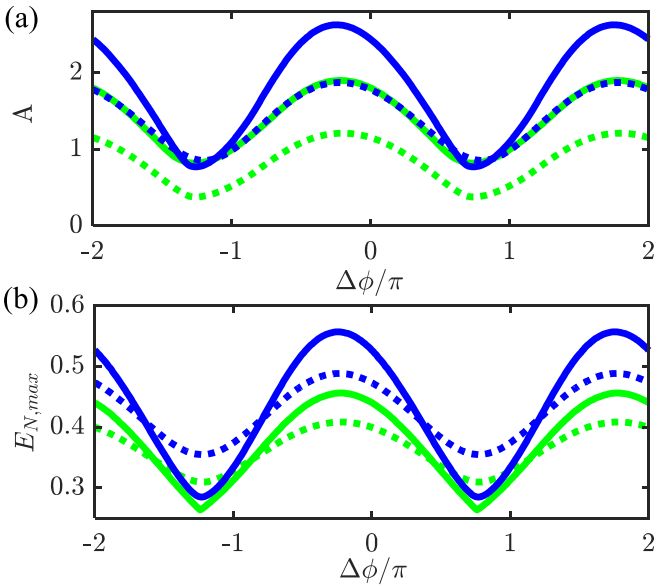

FIG. 3. (a) Cross-correlation area A and (b) light-oscillator entanglement $E_{N,\max}$ as a function of the relative phase $\Delta\phi$ for $(\epsilon_1, \Lambda)/\omega_m = (2\times10^4, 0.02)$ [green (light gray) dashed line], $(\epsilon_1, \Lambda)/\omega_m = (2\times10^4, 0.04)$ [green (light gray) solid line], $(\epsilon_1, \Lambda)/\omega_m = (4\times10^4, 0.02)$ [blue (dark gray) dashed line], and $(\epsilon_1, \Lambda)/\omega_m = (4\times10^4, 0.04)$ [blue (dark gray) solid line]. Other parameters are the same as in Fig. 2.

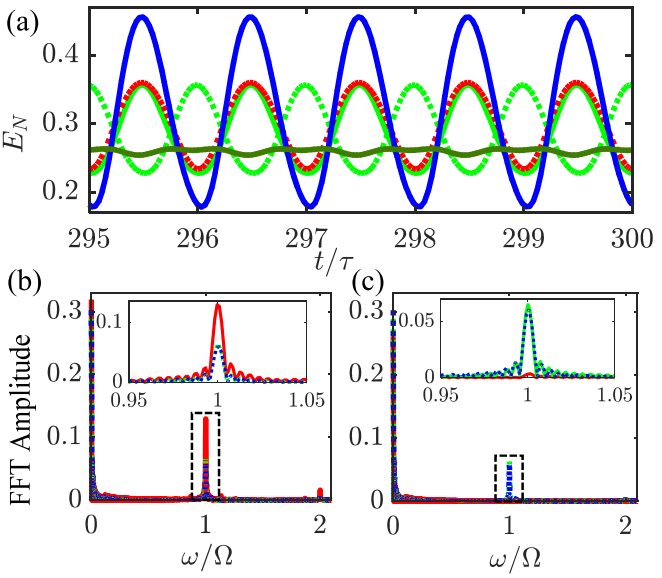

FIG. 4. (a) The long-time dynamics of the light-oscillator entanglement E_N for the set of parameters: $(\epsilon_1, \Lambda)/\omega_m = (0, 0.04)$, $\Delta\phi = -0.24\pi$ [green (light gray) solid line]; $(\epsilon_1, \Lambda)/\omega_m = (0, 0.04)$, $\Delta\phi = 0.76\pi$ [green (light gray) dashed line]; $(\epsilon_1, \Lambda)/\omega_m = (2\times10^4, 0)$, $\Delta\phi = -0.24\pi$ [red (dark gray) dashed line]; $(\epsilon_1, \Lambda)/\omega_m = (2\times10^4, 0.04)$, $\Delta\phi = -0.24\pi$ [blue (dark gray) solid line]; $(\epsilon_1, \Lambda)/\omega_m = (2\times10^4, 0.04)$, $\Delta\phi = 0.76\pi$ [cyan (gray) solid line]. (b),(c) Fast-Fourier-transform (FFT) analysis of the entanglement dynamics in the long-time limit for the in-phase ($\Delta\phi = -0.24\pi$, left panel) and the out-of-phase ($\Delta\phi = 0.76\pi$, right panel) modulations. The corresponding parameters of (b) and (c) are $(\epsilon_1, \Lambda)/\omega_m = (2\times10^4, 0.04)$ [red (dark gray) solid line], $(\epsilon_1, \Lambda)/\omega_m = (0, 0.04)$ [green (light gray) dashed line], $(\epsilon_1, \Lambda)/\omega_m = (2\times10^4, 0)$ [blue (dark gray) dashed line], and the insets are extractions of the zones around $\omega = \Omega$. Other parameters are the same as in Fig. 2.

enhancement of the optomechanical entanglement; see further discussion later in the paper.

With well-selected cooperative phases, we can now find the constructive and destructive interference patterns in optomechanical entanglement, as shown in Fig. 4. The steady-state entanglement dynamics, which exhibits a periodic behavior, can be described as a superposition of cosine functions via the Fourier expansion, giving rise to

$$E_N = E_0 + \sum_{n=1}^{\infty} E_n \cos(n\Omega t + \phi_n). \tag{20}$$

For the single-field driving cases with the parameters $(\epsilon_1, \Lambda)/\omega_m = (2\times10^4, 0)$ and $(\epsilon_1, \Lambda)/\omega_m = (0, 0.04)$, the time-dependent entanglements are approximately

$$E_{N,\epsilon_1} \approx 0.3 - 0.063\cos(\Omega t + 0.02) - 0.003\cos(2\Omega t - 0.56) \tag{21}$$

and

$$E_{N,\Lambda} \approx 0.29 - 0.065\cos(\Omega t + 0.021) + 0.005\cos(2\Omega t + 0.53), \tag{22}$$

respectively, where the effect of the DPA on both the classical and quantum dynamics of the system is already included. While the two-field driving scheme is implemented with $(\epsilon_1, \Lambda)/\omega_m = (2\times10^4, 0.04)$, the time-dependent entanglement becomes

$$E_N^{(c)} \approx 0.32 - 0.139\cos(\Omega t - 0.015) + 0.010\cos(2\Omega t + 1.35) \tag{23}$$

for $\Delta\phi = -0.24\pi$ (i.e., the constructive pattern), and

$$E_N^{(d)} \approx 0.26 + 0.004\cos(\Omega t + 0.23) - 0.002\cos(2\Omega t + 0.58) \tag{24}$$

for $\Delta\phi = 0.76\pi$ (i.e., the destructive pattern). The optomechanical entanglement under two-field driving can be approximately regarded as the superposition of the two cosinelike functions Eqs. (21) and (22) under individual single-field driving. However, the effects of amplitude-modulated driving and DPA pumping on the light-oscillator entanglement E_N are indeed different and can be outlined mainly in two aspects. First, the expectation value of E_N can be increased (decreased) for the constructive (destructive) phase for a sufficiently large DPA gain Λ, which changes the cavity amplitude even at zeroth-order according to $\langle a(t)\rangle \approx (\kappa - i\omega_m)\epsilon_0/(\kappa^2 + \omega_m^2 - 4\Lambda^2) + O(e^{\pm i2\omega_m t})$ [see Eq. (4)], while the modulation amplitude ϵ_1 of the cavity driving only has a small effect. Second, the oscillation amplitude for the time-periodic optomechanical entanglement can be more than twice that under individual modulation, as shown by the Fourier transform analysis of the steady-state dynamics. As for $E_N^{(c)}$, the amplitude of the Fourier component Ω is about 0.139, which is larger than twice the amplitudes in E_{N,ϵ_1} and $E_{N,\Lambda}$. This implies that the cooperative effect cannot be simply studied by

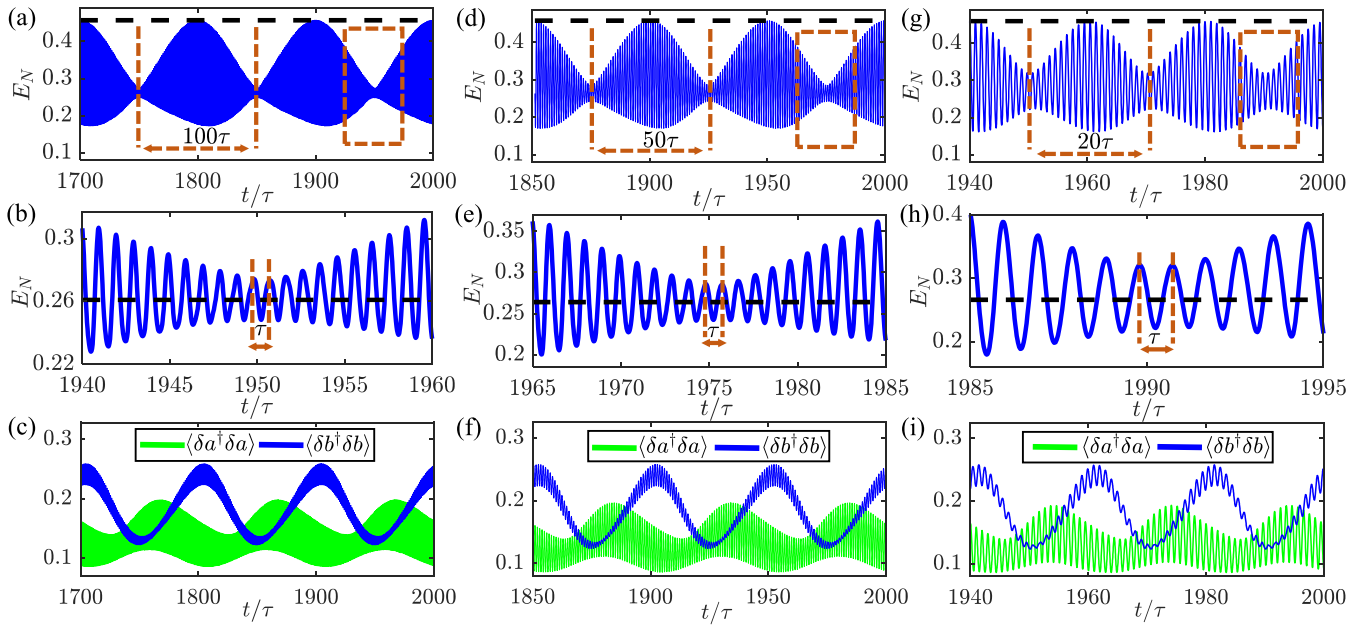

FIG. 5. Dynamical correspondence between the beating in light-oscillator entanglement E_N and the time evolutional mean photon number $\langle\delta a^\dagger\delta a\rangle$ [green (light gray) line] and phonon number $\langle\delta b^\dagger\delta b\rangle$ [blue (dark gray) line]. Parameters are as follows: the cavity driving strength $\epsilon_1/\omega_m = 2\times10^4$ and the DPA pumping $\Lambda/\omega_m = 0.04$, with $(\Omega, \Delta_p)/\omega_m = (1.99, 2.01)$ in (a)–(c), (1.98,2.02) in (d)–(f), and (1.95,2.05) in (g)–(i). The relative phase is set as $\Delta\phi = -0.24\pi$. The horizontal dashed lines indicate the dynamical maximum $E_{N,\max}$ of the light-oscillator entanglement in (a), (d), and (g), and the expectation values in the corresponding zoom-in figures (b), (e), and (h). Other parameters are the same as in Fig. 2.

two superposed cavity driving fields, and the quantum effect of the DPA may have additional significant influences; see further discussion later in the paper. We also note that there exists nonvanishing amplitude for the Fourier component 2Ω, because the time-dependent covariance matrix involves nonlinear high-order terms $\sim[\int_\tau^t dt'\mathcal{L}(t')]^n$, as predicted by Eq. (16).

The cooperative effect of the two drivings can be further evidenced by the beating of the optomechanical entanglement, as shown in Fig. 5, where the modulation frequencies of the cavity driving and of the DPA pumping are slightly shifted, e.g., $(\Omega, \Delta_p)/\omega_m = (1.99, 2.01)$ in Figs. 5(a)–5(c). For an arbitrary phase difference between the two driving fields (e.g., $\Delta\phi = -0.24\pi$), a periodic variation in the entanglement amplitude can be clearly seen with the period of the envelope being $2\pi/(\Delta_p - \Omega) = 100\tau$, 50τ, and 20τ, as indicated in Figs. 5(a), 5(d), and 5(g), respectively, and the frequency of the modulation is given by $\tau \equiv 2\pi/[(\Omega + \Delta_p)/2]$; see Figs. 5(b), 5(e), and 5(h). These are referred to as entanglement beating, which resemble the well-known interference pattern between two waves of slightly different frequencies. The maximum value $E_N \approx 0.459$ in Figs. 5(a), 5(d), and 5(g) and the expectation value $E_N \approx 0.264$ in Figs. 5(b), 5(e), and 5(h), as indicated by the horizontal dashed lines, are basically the peak E_N values of the constructive pattern and the destruction pattern; see the green (light gray) line in Fig. 3(b). It should be noted that a simple amplitude-modulated periodic driving (e.g., $\epsilon_1/\omega_m \neq 0$, $\Lambda/\omega_m = 0$) cannot produce a periodic envelope in the light-oscillator entanglement. In contrast, the optomechanical entanglement can be engineered with appropriately tuned two-field drivings.

Remarkably, as shown in Figs. 5(c), 5(f), and 5(i), the time dependence of the mean photon number $\langle\delta a^\dagger\delta a\rangle$ and phonon number $\langle\delta b^\dagger\delta b\rangle$ present the same oscillation period as the entanglement dynamics, manifesting the dynamical correspondence between the entanglement beating and the energy exchange between the optical and mechanical modes. This implies that a new degree of freedom for the dynamical control can be flexibly implemented with cooperative cavity driving and DPA pumping, which may find practical applications in CV quantum information processing, such as information storage and retrieval. Moreover, the entanglement beating can be detected by measuring the correlation between the cavity and mechanical modes. As suggested in [14], the quadratures of the cavity mode can be straightforwardly measured by homodyning the cavity output with an additional "probe" cavity mode, where all of the entries of the covariance matrix $V(t)$ used to calculate the logarithmic negativity E_N can be determined [14,17,31].

Finally, we examine how good the light-oscillator entanglement E_N can benefit from coherent modulation under the in-phase two-field driving, and we show the density plot of the dynamical maximum of the logarithmic negativity $E_{N,\max}$ versus the two modulation strengths Λ and ϵ_1 [see Fig. 6(a)]. To reveal the pure quantum effect of the DPA pumping induced by $M_1(t)$, we also show the density plot of E_N by assuming $M(t) = M_0(t)$. The scenario with $M_1(t) = 0$, as discussed before, corresponds to the interference enhanced dynamics induced by two phase-locked drivings. With regard to the implementation of the similar scheme involving only $M_0(t)$, the optomechanical entanglement E_N may be alternatively modified by using a specially modulated driving

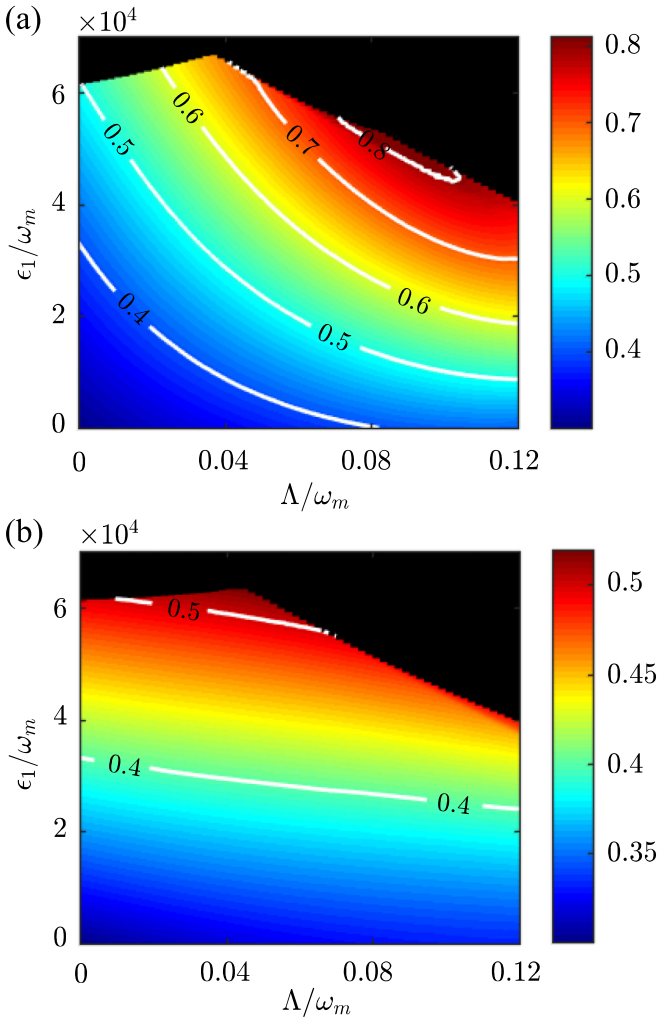

FIG. 6. Density plot of the light-oscillator entanglement $E_{N,\max}$ in the long-time limit vs the parametric gain Λ/ω_m and the modulation strength ϵ_1/ω_m with the relative phase $\Delta\phi = -0.24\pi$ for (a) $M_1(t) \neq 0$, (b) $M_1(t) = 0$. The black areas denote the unstable region confirmed by the Routh-Hurwitz criterion. The white contour lines denote the light-oscillator entanglement $E_{N,\max}$ of the different optimal values. Other parameters are the same as in Fig. 2.

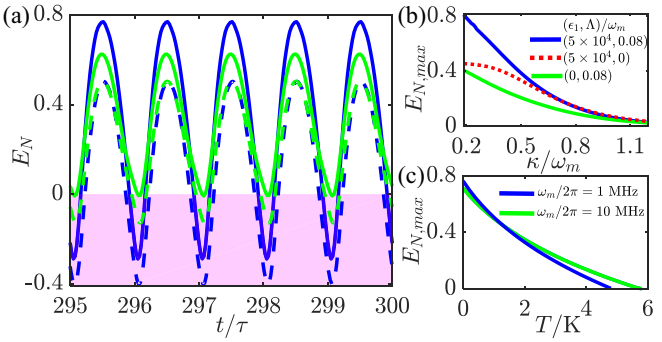

FIG. 7. (a) Time dependence of light-oscillator entanglement E_N in the long-time limit with the experimentally feasible parameters [66]: $L = 25$ mm, $F = 1.5 \times 10^4$, $\omega_m = 2\pi \times 1$ MHz, $Q = 10^6$, $m = 150$ ng, and the driving laser of the power $P_0 = 23.8$ mW (corresponding to $\epsilon_0/\omega_m = 9 \times 10^4$) and the wavelength $\lambda = 1064$ nm. Other parameter are $(\epsilon_1, \Lambda)/\omega_m = (3 \times 10^4, 0.08)$ [green (light gray) line], $(\epsilon_1, \Lambda)/\omega_m = (5 \times 10^4, 0.08)$ [blue (dark gray) line]. The thermal temperature for the solid lines is $T = 0$, while for the green (light gray) dashed line and the blue (dark gray) dashed line are $T = 1$ and 0.5 K, respectively. The relative phase is set as $\Delta\phi = -0.24\pi$. The red region below zero implies there is no entanglement between the mechanical and cavity modes. (b) The optimal steady entanglement $E_{N,\max}$ vs the cavity decay κ/ω_m for $(\epsilon_1, \Lambda)/\omega_m = (5 \times 10^4, 0.08)$ [blue (dark gray) line], $(\epsilon_1, \Lambda)/\omega_m = (5 \times 10^4, 0)$ [red (dark gray) dashed line], and $(\epsilon_1, \Lambda)/\omega_m = (0, 0.08)$ [green (light gray) line], respectively. $E_{N,\max}$ is optimized by choosing the appropriate relative phases for different cavity decay rates κ/ω_m. (c) The optimal steady entanglement $E_{N,\max}$ vs thermal temperature T for the set of parameters in (a) [blue (dark gray) line], and with the revised mechanical frequency $\omega_m/2\pi = 10$ MHz and decoherent rates $(\kappa, \gamma_m)/\omega_m = (0.25, 10^{-5})$ given by Ref. [69] [green (light gray) line]. The cavity driving and DPA pumping strengths for the latter case are $(\epsilon_0, \epsilon_1, \Lambda)/\omega_m = (9 \times 10^4, 5 \times 10^4, 0.08)$.

or parametric pumping. However, the situation can be very different while the two fields are applied simultaneously. In comparison, we find that the periodic modulation of the cavity quadratures can slightly modify the stability region (justified by the Routh-Hurwitz criterion). More importantly, it can strongly improve the optomechanical entanglement, leading to an optimal $E_{N,\max}$ as large as 0.8, which appears at the parameter regime with large cavity driving strength and parametric gain (i.e., the upper right corner of the plot), manifesting again the cooperative effect of the two drivings. Without $M_1(t)$, the dynamical optomechanical entanglement can only reach the upper bound about 0.5 with the system being in the vicinity of the instability, which corresponds to the scenario that the optomechanical cavity is simply driven by two classical fields with same frequency and different strengths ϵ_1, $2\Lambda\epsilon_0/\sqrt{\kappa^2 + \Delta_0^2}$. By applying the cooperative driving scheme, $E_{N,\max} = 0.5$ can be readily accessed with the system being far away from the unstable region.

Furthermore, while the scheme is implemented by the state-of-the-art experimental setup [66], which also works in the resolved sideband regime for $\kappa/2\pi = c/4FL = 0.2$ MHz (i.e., $\kappa/\omega_m = 0.2$), we find that the cooperative optomechanical entanglement is strongly robust against the thermal noise, as shown in Fig. 7(a). The optimal dynamical E_N can be achieved by strengthening the cooperative drivings, but the increasing oscillation amplitude may also lead to periodic vanishing of the optomechanical entanglement (denoted by $E_N < 0$) at some time intervals, which is known to be the entanglement sudden death and revival [25] and is of general interest in quantum physics [67,68]. As a result, the optimal optomechanical entanglement remains higher than 0.5 for the thermal temperature being as high as 1 K for $(\epsilon_1, \Lambda)/\omega_m = (5 \times 10^4, 0.08)$ [blue (dark gray) dashed line] and being 0.5 K for $(\epsilon_1, \Lambda)/\omega_m = (3 \times 10^4, 0.08)$ [green (light gray) dashed line], which cannot be accessed by the two classical drivings scheme mentioned before, and therefore manifests itself as the unique signature of the cooperative effect under the cavity driving and the DPA pumping.

While the cavity decay rate increases and approaches the bad cavity limit [see Fig. 7(b)], we find that the cooperative

two-field driving scheme is superior to the cases under individual driving for $\kappa/\omega_m < 0.6$, while for the system that is far away from the resolved sideband limit $\kappa/\omega_m \sim 1$, the optomechanical entanglement for all schemes tends to be the same and be vanishing. In addition, we plot the light-oscillator entanglement $E_{N,\max}$ versus the thermal temperature T, and we find the critical temperature $T_c = 4.7$ K where $E_{N,\max}$ vanishes. In comparison with the scheme where the DPA is replaced by an atomic media and the critical temperature is $T \approx 3$ K [69], we note that the two-field driving scheme here can generate strong entanglement ($E_{N,\max} \sim 0.25$) even at $T \approx 3$ K and has a larger critical temperature $T = 5.8$ K with the same cavity and mechanical parameters; see the green (light gray) line in Fig. 7(c).

V. CONCLUSION

In conclusion, we have demonstrated strong light-mechanical entanglement in an optomechanical system subject to two cooperative laser drivings, namely the periodically amplitude-modulated cavity driving and the detuned DPA pumping. The cooperative effects of the two laser drivings are studied in both the classical and quantum dynamics. We find interesting interference patterns and beating in light-oscillator entanglement due to cooperative effects of the two drivings, which can alternatively be evidenced by the correlation spectra of the optical and mechanical modes. The optomechanical entanglement is greatly enhanced and goes beyond the regime attainable with simply two classical cavity drivings. The cooperation-based driving scheme is robust against the thermal noise and offers a versatile platform for practical applications of the modulated optomechanical system in quantum information processing, in particular for its merits in flexible control of the optomechanical energy transfer.

ACKNOWLEDGMENTS

This work is supported by the National Natural Science Foundation of China under Grants No. 11774058, No. 11674060, No. 11874114, No. 11875108, and No. 11705030, the Natural Science Foundation of Fujian Province under Grant No. 2017J01401, and the Qishan fellowship of Fuzhou University.

APPENDIX: A

In the presence of strong external driving, we can rewrite each Heisenberg operator as $O = \langle O(t)\rangle + \delta O$ ($O = q,\ p,\ a$) [where δO are quantum fluctuation operators with zero-mean around the c-number mean values $\langle O(t)\rangle$], and justify that $\langle a^\dagger(t)a(t)\rangle \simeq |\langle a(t)\rangle|^2$ and $\langle a(t)q(t)\rangle \simeq \langle a(t)\rangle\langle q(t)\rangle$ are good approximations. Applying the standard linearization techniques to the QLEs in Eq. (2), we thus obtain the following set of equations for the mean values [14]:

$$\begin{aligned}
\langle \dot{q}(t)\rangle &= \omega_m \langle p(t)\rangle,\\
\langle \dot{p}(t)\rangle &= -\omega_m\langle q(t)\rangle - \gamma_m\langle p(t)\rangle + \sqrt{2}g|\langle a(t)\rangle|^2,\\
\langle \dot{a}(t)\rangle &= -(\kappa + i\Delta_0)\langle a(t)\rangle + i\sqrt{2}g\langle a(t)\rangle\langle q(t)\rangle\\
&\quad + \epsilon(t) + 2\Lambda e^{i\theta}\langle a(t)\rangle^* e^{-i\Delta_p t}.
\end{aligned} \tag{A1}$$

When the system is far away from the optomechanical instabilities and multistabilities [36], the semiclassical dynamics [i.e., the asymptotic solutions of Eq. (A1)] here will evolve toward a fixed periodic orbit with the same periodicity of the modulation τ, which can be treated perturbatively since the only two nonlinear terms in Eq. (A1) are both proportional to $\sqrt{2}g$ and $\sqrt{2}g \ll \omega_m$. Thus it is reasonable to perform a double expansion of the asymptotic solution $\langle O(t)\rangle$ in the powers of the coupling constant $\sqrt{2}g$ and in terms of the Fourier components [36]

$$\begin{aligned}
\langle O(t)\rangle &= \sum_{n=-\infty}^{\infty} O_n e^{in\Omega t}\\
&= \sum_{j=0}^{\infty}\sum_{n=-\infty}^{\infty} O_{n,\,j} e^{in\Omega t}(\sqrt{2}g)^j.
\end{aligned} \tag{A2}$$

Substituting Eq. (A2) into Eq. (A1), we readily obtain the time-independent coefficients $O_{n,\,j}$, which fulfill the following recursive formulas. For $j = 0$,

$$\begin{aligned}
&p_{n,0} = 0,\ q_{n,0} = 0,\\
&a_{1,0} = \frac{[\kappa - i(\Delta_0 - 2\Omega)]\epsilon_1 e^{-i\varphi}}{[\kappa - i(\Delta_0 - 2\Omega)][\kappa + i(\Delta_0 + \Omega)] - 4\Lambda^2},\\
&a_{0,0} = \frac{[\kappa - i(\Delta_0 - \Omega)]\epsilon_0 + 2\Lambda\epsilon_1 e^{i(\theta+\varphi)}}{[\kappa - i(\Delta_0 - \Omega)](\kappa + i\Delta_0) - 4\Lambda^2},\\
&a_{-1,0} = \frac{(\kappa - i\Delta_0)\epsilon_1 e^{i\varphi} + 2\Lambda e^{i\theta}\epsilon_0}{(\kappa - i\Delta_0)[\kappa + i(\Delta_0 - \Omega)] - 4\Lambda^2},
\end{aligned} \tag{A3}$$

with $a_{n,0} = 0$ ($n \neq 0, \pm 1$). And for $j \geqslant 1$,

$$\begin{aligned}
q_{n,j} &= \omega_m \sum_{k=0}^{j-1}\sum_{m=-\infty}^{\infty} \frac{a^*_{m,k}a_{n+m,j-k-1}}{\omega_m^2 - (n\Omega)^2 + i\gamma_m n\Omega},\\
p_{n,j} &= \frac{in\Omega}{\omega_m} q_{n,j},\\
a_{n,j} &= \frac{2\Lambda e^{i\theta}a^*_{-n-1,j}}{\kappa + i(\Delta_0 + n\Omega)} + i\sum_{k=0}^{j-1}\sum_{m=-\infty}^{\infty} \frac{a_{m,k}q_{n-m,j-k-1}}{\kappa + i(\Delta_0 + n\Omega)}.
\end{aligned} \tag{A4}$$

The analytical solutions of Eq. (A3) are similar in Ref. [36]. Without amplitude-modulated driving ($\epsilon_1/\omega_m = 0$), Eq. (A3) can be simplified into

$$\begin{aligned}
&p_{n,0} = 0,\ q_{n,0} = 0,\\
&a_{0,0} = \frac{[\kappa - i(\Delta_0 - \Omega)]\epsilon_0}{[\kappa - i(\Delta_0 - \Omega)](\kappa + i\Delta_0) - 4\Lambda^2},\\
&a_{-1,0} = \frac{2\Lambda e^{i\theta}\epsilon_0}{[\kappa + i(\Delta_0 - \Omega)](\kappa - i\Delta_0) - 4\Lambda^2}.
\end{aligned} \tag{A5}$$

And when DPA is absent ($\Lambda/\omega_m = 0$), Eq. (A3) can be expressed as

$$\begin{aligned}
&p_{n,0} = 0,\ q_{n,0} = 0,\\
&a_{0,0} = \frac{\epsilon_0}{\kappa + i\Delta_0},\\
&a_{-1,0} = \frac{\epsilon_1 e^{-i\varphi}}{\kappa + i(\Delta_0 - \Omega)},\\
&a_{1,0} = \frac{\epsilon_1 e^{-i\varphi}}{\kappa + i(\Delta_0 + \Omega)}.
\end{aligned} \tag{A6}$$

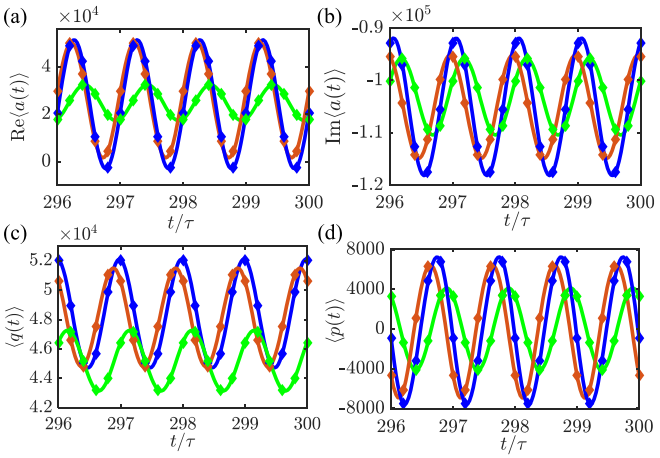

FIG. 8. Time evolution of the classical mean values of the cavity and mechanical modes for $(\epsilon_1, \Lambda)/\omega_m = (2 \times 10^4, 0)$ [red (gray) line], $(\epsilon_1, \Lambda)/\omega_m = (0, 0.04)$ [green (light gray) line], and $(\epsilon_1, \Lambda)/\omega_m = (2 \times 10^4, 0.04)$ [blue (dark gray) line], respectively. The lines are numerical simulations with Eq. (A1) and the markers correspond to the analytical solutions Eq. (A2). Other parameters are the same as in Fig. 2 except $\varphi = \theta = 0$. Under this parameter regime, the laser detuning from the cavity resonance is modified approximately by $\bar{\delta}/\omega_m \equiv -\sqrt{2}g\langle q(t)\rangle \simeq -0.2$ due to the mechanical displacement.

By truncating the series to the first terms with indexes $j \leqslant 18$ and $n = -1, 0, 1$, we find that the obtained analytical approximations for the asymptotic mean values $\langle O(t)\rangle$ are in good agreement with the numerical results shown in Fig. 8. Thus, it becomes convenient to evaluate the linearized quantum dynamics with high accuracy by using the truncated Fourier expansions (A2). In addition, the correlation spectrum is calculated based on the analytical solutions.

APPENDIX: B

Here we investigate the effect of either amplitude-modulated driving or DPA on the correlation spectrum and entanglement dynamics. When only the amplitude-modulated driving is considered with $(\epsilon_1, \Lambda)/\omega_m = (2 \times 10^4, 0)$, we show the imaginary part, the real part, and the modulus of correlation spectra $S(\omega)$ versus the normalized frequency ω/ω_m, respectively, in Figs. 9(a), 9(b), and 9(c). One can see that the imaginary and real parts of $S(\omega)$ as well as the time evolutional entanglement E_N [see Fig. 2(d)] reverse when the phase of the driving laser φ is π, but the modulus of $S(\omega)$ and maximum light-mechanical entanglement $E_{N,\max}$ are the same for different phases φ. Thus, when the amplitude-modulated driving is individually applied, the dynamical entanglement can be translationally shifted by controlling the driving phase φ. Similarly, when the DPA pumping is individually applied, the dynamical entanglement can be translationally shifted by controlling the parametric phase θ [e.g., $(\epsilon_1, \Lambda)/\omega_m = (0, 0.04)$], as shown in Fig. 10.

Furthermore, we plot the time evolution of E_N in Fig. 9(d) for different modulation amplitudes $\epsilon_1/\omega_m = 1 \times 10^4$ [green (light gray) solid line], 2×10^4 [red (dark gray) dashed line], and 3×10^4 [blue (dark gray) solid line] when the DPA is

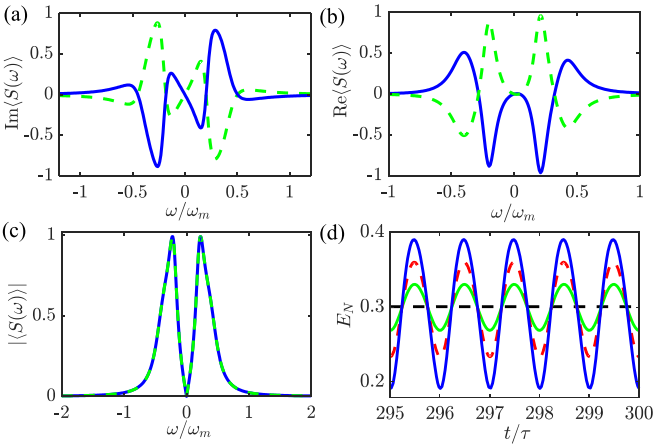

FIG. 9. (a) Imaginary part, (b) real part, (c) and modulus of the correlation spectra $S(\omega)$ vs the normalized frequency ω/ω_m with $(\epsilon_1, \Lambda)/\omega_m = (2 \times 10^4, 0)$ as well as $\varphi = 0$ [blue (dark gray) solid line] and $\varphi = \pi$ [green (light gray) dashed line]. (d) Light-mechanical entanglement E_N vs evolution time t for the different modulation amplitudes $\epsilon_1/\omega_m = 1 \times 10^4$ [green (light gray) solid line], 2×10^4 [red (dark gray) dashed line], and 3×10^4 [blue (dark gray) solid line] with $\varphi = 0$ and $\Lambda/\omega_m = 0$. Other parameters are the same as in Fig. 2.

absent $(\Lambda/\omega_m = 0)$. The light-oscillator entanglement $E_{N,\max}$ is increased with the increasing of the modulation amplitude ϵ_1. On the other hand, when the amplitude-modulated driving is absent $(\epsilon_1/\omega_m = 0)$, increasing the parametric gain Λ can also enhance $E_{N,\max}$, as seen in Fig. 10(d), in which the time evolutions of E_N are, respectively, plotted for the different parametric gain $\Lambda/\omega_m = 0.02$ [green (light gray) solid line], 0.04 [red (dark gray) dashed line], and 0.06 [blue (dark gray) solid line].

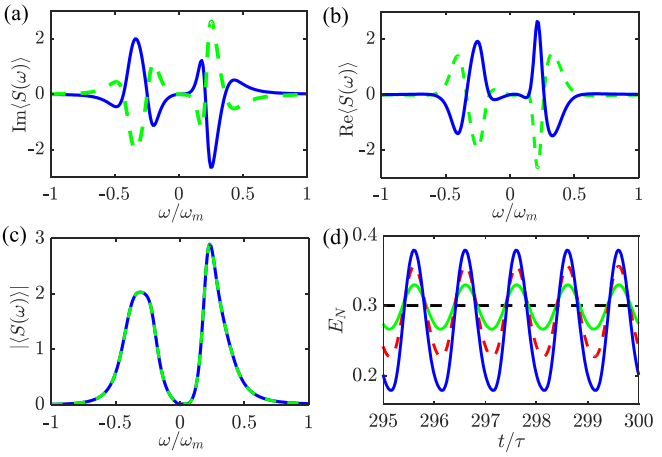

FIG. 10. (a) The imaginary part, (b) real part, and (c) modulus of the correlation spectra $S(\omega)$ vs the normalized frequency ω/ω_m with $(\epsilon_1, \Lambda)/\omega_m = (0, 0.04)$ as well as $\theta = 0$ [blue (dark gray) solid line] and $\theta = \pi$ [green (light gray) dashed line]. (d) Light-mechanical entanglement E_N vs evolution time t for the different parametric gain $\Lambda/\omega_m = 0.02$ [green (light gray) solid line], 0.04 [red (dark gray) dashed line], and 0.06 [blue (dark gray) solid line] with $\theta = 0$ and $\epsilon_1/\omega_m = 0$. Other parameters are the same as in Fig. 2.

[1] A. Einstein, B. Podolsky, and N. Rosen, Can quantum-mechanical description of physical reality be considered complete? Phys. Rev. **47**, 777 (1935).

[2] L. M. Duan, G. Giedke, J. I. Cirac, and P. Zoller, Inseparability Criterion for Continuous Variable Systems, Phys. Rev. Lett. **84**, 2722 (2000).

[3] W. P. Bowen, R. Schnabel, P. K. Lam, and T. C. Ralph, Experimental Investigation of Criteria for Continuous Variable Entanglement, Phys. Rev. Lett. **90**, 043601 (2003).

[4] J. Eisert, and M. B. Plenio, Introduction to the basics of entanglement theory in continuous-variable systems, Int. J. Quantum Inf. **1**, 479 (2003).

[5] S. L. Braunstein, and P. Van Loock, Quantum information with continuous variables, Rev. Mod. Phys. **77**, 513 (2005).

[6] M. D. Reid, P. D. Drummond, W. P. Bowen, E. G. Cavalcanti, P. K. Lam, H. A. Bachor, U. L. Andersen, and G. Leuchs, Colloquium: The Einstein-Podolsky-Rosen paradox: From concepts to applications, Rev. Mod. Phys. **81**, 1727 (2009).

[7] U. L. Andersen, G. Leuchs, and C. Silberhorn, Continuous-variable quantum information processing, Laser Photon. Rev. **4**, 337 (2010).

[8] M. Schmidt, M. Ludwig, and F. Marquardt, Optomechanical circuits for nanomechanical continuous variable quantum state processing, New J. Phys. **14**, 125005 (2012).

[9] O. Arcizet, P. F. Cohadon, T. Briant, and A. Heidmann, Radiation-pressure cooling and optomechanical instability of a micro-mirror, Nature (London) **444**, 71 (2006).

[10] F. Marquardt, J. P. Chen, A. A. Clerk, and S. M. Girvin, Quantum Theory of Cavity-Assisted Sideband Cooling of Mechanical Motion, Phys. Rev. Lett. **99**, 093902 (2007).

[11] I. Wilson-Rae, N. Nooshi, W. Zwerger, and T. J. Kippenberg, Theory of Ground State Cooling of a Mechanical Oscillator using Dynamical Backaction, Phys. Rev. Lett. **99**, 093901 (2007).

[12] A. A. Clerk, F. Marquardt, and K. Jacobs, Back-action evasion and squeezing of a mechanical resonator using a cavity detector, New J. Phys. **10**, 095010 (2008).

[13] M. Aspelmeyer, T. J. Kippenberg, and F. Marquardt, Cavity optomechanics, Rev. Mod. Phys. **86**, 1391 (2014).

[14] D. Vitali, S. Gigan, A. Ferreira, H. R. Böhm, P. Tombesi, A. Guerreiro, V. Vedral, A. Zeilinger, and M. Aspelmeyer, Optomechanical Entanglement between a Movable Mirror and a Cavity Field, Phys. Rev. Lett. **98**, 030405 (2007).

[15] C. Genes, A. Mari, P. Tombesi, and D. Vitali, Robust entanglement of a micromechanical resonator with output optical fields, Phys. Rev. A **78**, 032316 (2008).

[16] P. Sekatski, M. Aspelmeyer, and N. Sangouard, Macroscopic Optomechanics from Displaced Single-Photon Entanglement, Phys. Rev. Lett. **112**, 080502 (2014).

[17] G. D. Chiara, M. Paternostro, and G. M. Palma, Entanglement detection in hybrid optomechanical systems, Phys. Rev. A **83**, 052324 (2014).

[18] G. L. Wang, L. Huang, Y. C. Lai, and C. Grebogi, Nonlinear Dynamics and Quantum Entanglement in Optomechanical Systems, Phys. Rev. Lett. **112**, 110406 (2014).

[19] J. I. Cirac, P. Zoller, H. J. Kimble, and H. Mabuchi, Quantum State Transfer and Entanglement Distribution among Distant Nodes in a Quantum Network, Phys. Rev. Lett. **78**, 3221 (1997).

[20] J. Zhang, K. Peng, and S. L. Braunstein, Quantum-state transfer from light to macroscopic oscillators, Phys. Rev. A **68**, 013808 (2003).

[21] V. Fiore, Y. Yang, M. C. Kuzyk, R. Barbour, L. Tian, and H. Wang, Storing Optical Information as a Mechanical Excitation in a Silica Optomechanical Resonator, Phys. Rev. Lett. **107**, 133601 (2011).

[22] T. A. Palomaki, J. W. Harlow, J. D. Teufel, R. W. Simmonds, and K. W. Lehnert, Coherent state transfer between itinerant microwave fields and a mechanical oscillator, Nature (London) **495**, 210 (2013).

[23] S. Mancini, V. Giovannetti, D. Vitali, and T. Paolo, Entangling Macroscopic Oscillators Exploiting Radiation Pressure, Phys. Rev. Lett. **88**, 120401 (2002).

[24] S. M. Huang, and G. S. Agarwal, Entangling nanomechanical oscillators in a ring cavity by feeding squeezed light, New J. Phys. **11**, 103044 (2009).

[25] C. Joshi, J. Larson, M. Jonson, E. Andersson, and P. Öhberg, Entanglement of distant optomechanical systems, Phys. Rev. A **85**, 033805 (2012).

[26] Y. D. Wang, and A. A. Clerk, Reservoir-Engineered Entanglement in Optomechanical Systems, Phys. Rev. Lett. **110**, 253601 (2013).

[27] X. W. Xu, Y. J. Zhao, and Y. X. Liu, Entangled-state engineering of vibrational modes in a multimembrane optomechanical system, Phys. Rev. A **88**, 022325 (2013).

[28] J. Q. Liao, Q. Q. Wu, and F. Nori, Entangling two macroscopic mechanical mirrors in a two-cavity optomechanical system, Phys. Rev. A **89**, 014302 (2014).

[29] Y. D. Wang, S. Chesi, and A. A. Clerk, Bipartite and tripartite output entanglement in three-mode optomechanical systems, Phys. Rev. A **91**, 013807 (2015).

[30] C. J. Yang, J. H. An, W. L. Yang, and Y. Li, Generation of stable entanglement between two cavity mirrors by squeezed-reservoir engineering, Phys. Rev. A **92**, 062311 (2015).

[31] J. Li, I. M. Haghighi, N. Malossi, S. Zippilli, and D. Vitali, Generation and detection of large and robust entanglement between two different mechanical resonators in cavity optomechanics, New J. Phys. **17**, 103037 (2015).

[32] J. Li, G. Li, S. Zippilli, D. Vitali, and T. C. Zhang, Enhanced entanglement of two different mechanical resonators via coherent feedback, Phys. Rev. A **95**, 043819 (2017).

[33] R. Riedinger, A. Wallucks, I. Marinkovic, C. Löschnauer, M. Aspelmeyer, S. Hong, and S. Gröblacher, Remote quantum entanglement between two micromechanical oscillators, Nature (London) **556**, 473 (2018).

[34] W. J. Gu, G. X. Li, S. P. Wu, and Y. P. Yang, Generation of nonclassical states of mirror motion in the single-photon strong-coupling regime, Opt. Express **22**, 18254 (2014).

[35] G. Yu. Kryuchkyan, A. R. Shahinyan, and I. A. Shelykh, Quantum statistics in a time-modulated exciton-photon system, Phys. Rev. A **93**, 043857 (2016).

[36] A. Mari and J. Eisert, Gently Modulating Optomechanical Systems, Phys. Rev. Lett. **103**, 213603 (2009).

[37] A. Szorkovszky, A. C. Doherty, G. I. Harris, and W. P. Bowen, Mechanical Squeezing Via Parametric Amplification and Weak Measurement, Phys. Rev. Lett. **107**, 213603 (2011).

[38] A. Szorkovszky, G. A. Brawley, A. C. Doherty, and W. P. Bowen, Strong Thermomechanical Squeezing Via Weak Measurement, Phys. Rev. Lett. **110**, 184301 (2013).

[39] A. Szorkovszky, A. A. Clerk, A. C. Doherty, and W. P. Bowen, Detuned mechanical parametric amplification as a quantum non-demolition measurement, New J. Phys. **16**, 043023 (2014).

[40] B. A. Levitan, A. Metelmann, and A. A. Clerk, Optomechanics with two-phonon driving, New J. Phys. **18**, 093014 (2016).
[41] G. S. Agarwal, and S. M. Huang, Strong mechanical squeezing and its detection, Phys. Rev. A **93**, 043844 (2016).
[42] H. H. Adamyan, J. A. Bergou, N. T. Gevorgyan, and G. Y. Kryuchkyan, Strong squeezing in periodically modulated optical parametric oscillators, Phys. Rev. A **92**, 053818 (2015).
[43] C. S. Hu, Z. B. Yang, H. Z. Wu, Y. Li, and S. B. Zheng, Twofold mechanical squeezing in a cavity optomechanical system, Phys. Rev. A **98**, 023807 (2018).
[44] A. Mari, and J. Eisert, Opto- and electro-mechanical entanglement improved by modulation, New J. Phys. **14**, 075014 (2012).
[45] R. X. Chen, L. T. Shen, Z. B. Yang, H. Z. Wu, and S. B. Zheng, Enhancement of entanglement in distant mechanical vibrations via modulation in a coupled optomechanical system, Phys. Rev. A **89**, 023843 (2014).
[46] M. Abdi, and M. J. Hartmann, Entangling the motion of two optically trapped objects via time-modulated driving field, New J. Phys. **17**, 013056 (2015).
[47] M. Wang, X. Y. Lü, Y. D. Wang, J. Q. You, and Y. Wu, Macroscopic quantum entanglement in modulated optomechanics, Phys. Rev. A **94**, 053807 (2016).
[48] C. G. Liao, R. X. Chen, H. Xie, and X. M. Lin, Reservoir-engineered entanglement in a hybrid modulated three-mode optomechanical system, Phys. Rev. A **97**, 042314 (2018).
[49] W. J. Gu, Z. Yi, L. H. Sun, and Y. Yan, Generation of mechanical squeezing and entanglement via mechanical modulations, Opt. Express **26**, 30773 (2018).
[50] C. S. Hu, L. T. Shen, Z. B. Yang, H. Z. Wu, Y. Li, and S. B. Zheng, Manifestation of classical nonlinear dynamics in optomechanical entanglement with a parametric amplifier, Phys. Rev. A **100**, 043824 (2019).
[51] H. P. Breuer, M. Holthaus, and K. Dietz, The role of avoided crossings in the dynamics of strong laser field-matter interactions, Z. Phys. D **8**, 349 (1988).
[52] H. J. Briegel and S. Popescu, Entanglement and intra-molecular cooling in biological systems? A quantum thermodynamic perspective, arXiv:0806.4552.
[53] A. Farace, and V. Giovannetti, Enhancing quantum effects via periodic modulations in optomechanical systems, Phys. Rev. A **86**, 013820 (2012).
[54] S. M. Huang, and G. S. Agarwal, Enhancement of cavity cooling of a micromechanical mirror using parametric interactions, Phys. Rev. A **79**, 013821 (2009).
[55] X. Y. Lü, Y. Wu, J. R. Johansson, H. Jing, J. Zhang, and F. Nori, Squeezed Optomechanics with Phase-Matched Amplification and Dissipation, Phys. Rev. Lett. **114**, 093602 (2015).
[56] V. S. Malinovsky and I. R. Sola, Quantum Phase Control of Entanglement, Phys. Rev. Lett. **93**, 190502 (2004).
[57] V. S. Malinovsky and I. R. Sola, Phase-Controlled Collapse and Revival of Entanglement of Two Interacting Qubits, Phys. Rev. Lett. **96**, 050502 (2006).
[58] V. S. Malinovsky, I. R. Sola, and J. Vala, Phase-controlled two-qubit quantum gates, Phys. Rev. A **89**, 032301 (2014).
[59] B. Y. Chang, I. R. Sola, and V. S. Malinovsky, Anomalous Rabi Oscillations in Multilevel Quantum Systems, Phys. Rev. Lett. **120**, 133201 (2018).
[60] C. W. Gardiner, and P. Zoller, *Quantum Noise*, 3rd ed. (Springer, New York, 2004).
[61] Z. J. Deng, S. J. M. Habraken, and F. Marquardt, Entanglement rate for Gaussian continuous variable beams, New J. Phys. **18**, 063022 (2016).
[62] X. B. Yan, Enhanced output entanglement with reservoir engineering, Phys. Rev. A **96**, 053831 (2017).
[63] G. Teschl, *Ordinary Differential Equations and Dynamical Systems* (American Mathematical Society, Providence, RI, 2012).
[64] G. Adesso, A. Serafini, and F. Illuminati, Extremal entanglement and mixedness in continuous variable systems, Phys. Rev. A **70**, 022318 (2004).
[65] E. X. DeJesus and C. Kaufman, Routh-Hurwitz criterion in the examination of eigenvalues of a system of nonlinear ordinary differential equations, Phys. Rev. A **35**, 5288 (1987).
[66] S. J. B. Hertzberg, M. R. Vanner, G. D. Cole, S. Gigan, K. C. Schwab, and M. Aspelmeyer, Demonstration of an ultracold micro-optomechanical oscillator in a cryogenic cavity, Nat. Phys. **5**, 485 (2009).
[67] T. Yu and J. H. Eberly, Finite-Time Disentanglement Via Spontaneous Emission, Phys. Rev. Lett. **93**, 140404 (2004).
[68] T. Yu and J. H. Eberly, Sudden death of entanglement, Science **323**, 598 (2009).
[69] C. Genes, D. Vitali, and P. Tombesi, Emergence of atom-light-mirror entanglement inside an optical cavity, Phys. Rev. A **77**, 022318(R) (2008).